

Adsorption of alkanes, alkenes, and their mixtures in single-walled carbon nanotubes and bundles

| | |
|-------------------------------|--|
| Journal: | <i>Molecular Simulation/Journal of Experimental Nanoscience</i> |
| Manuscript ID: | GMOS-2008-0099.R1 |
| Journal: | Molecular Simulation |
| Date Submitted by the Author: | 21-Jul-2008 |
| Complete List of Authors: | Jakobtorweihen, Sven; Hamburg University of Technology, Institute of Chemical Reaction Engineering Keil, Frerich J.; Hamburg University of Technology, Institute of Chemical Reaction Engineering |
| Keywords: | carbon nanotubes, adsorption, alkanes, alkenes, molecular simulations |
| | |

SCHOLARONE™
Manuscripts

Adsorption of alkanes, alkenes, and their mixtures in single-walled carbon nanotubes and bundles

S. Jakobtorweihen and F. J. Keil*

*Hamburg University of Technology, Institute of Chemical Reaction Engineering,
Eissendorfer Str. 38, D-21073 Hamburg, Germany*

Abstract

Monte Carlo simulations are employed to calculate pure component adsorption isotherms of linear alkanes (C₂–C₁₂), alkenes (C₂–C₄), and some of their binary mixtures (ethane-ethene, propane-propene, *cis*-2-butene-*trans*-2-butene, propene-1-butene) in single-walled carbon nanotubes. The zigzag structures of carbon nanotubes of various diameters ((10,0), (20,0), (30,0), and (40,0)) are used. Furthermore, Henry coefficients and isosteric heats of adsorption are calculated. The dependence of these properties as a function of chain length (carbon number) is presented. The relation of the critical parameters and the isosteric heats of adsorption, observed earlier for zeolites, could be confirmed for carbon nanotubes. The adsorption behaviour of 1-butene, *cis*-2-butene, and *trans*-2-butene are compared in detail. Radial density profiles of 1-butene in a (40,0) nanotube for various pressures reveal a built-up of three layers inside the pores with increasing pressure. For all investigated binary mixtures, one of the component isotherms shows a distinct maximum owing to an entropic effect and non-idealities of the bulk gas phase behaviour. Additionally, adsorption in carbon nanotube bundles in hexagonal arrangement is studied. Depending on the pore arrangements, pore diameters, and pressures, a fraction of the adsorbed gases is located in the interstitial space.

Keywords: carbon nanotube; adsorption; alkanes; alkenes; molecular simulations

* corresponding author, e-mail: keil@tu-harburg.de

1. INTRODUCTION

After the discovery of carbon nanotubes (CNTs) by Iijima [1], these materials were considered for adsorption of various gases. Besides hydrocarbons [2–6], adsorption of other molecules and mixtures on single-walled carbon nanotubes (SWCNTs) were investigated, like hydrogen [7–9], nitrogen [10–13], nitrogen/oxygen [14, 15], water [16], neon [17], helium [18], and xenon [19]. Cao *et al.* [3] investigated the adsorption of methane on triangular arrays of SWCNTs at room temperature with the grand canonical Monte Carlo (GCMC) method. The carbon atoms on the tubular wall were structured according to the armchair arrangement, and the “site-to-site method” was used to calculate the interaction between a methane molecule inside the tube and a carbon atom on the tubular wall. The gap between the tubes was varied in order to find the optimum gap with respect to the amount of adsorbed methane. Jiang *et al.* [4] studied adsorption and separation of linear (C1–C5) and branched (C5 isomers) alkanes on (10,10) SWCNT bundles at 300 K using configurational-bias Monte Carlo (CBMC) simulations. For pure linear alkanes, the limiting adsorption properties at zero coverage exhibit a linear relation with the alkane carbon number; long alkanes are more adsorbed at low pressures, but the reverse is found for short alkanes at high pressures. For pure branched alkanes, the linear isomer adsorbs to a greater extent than its branched counterparts. For a five-component mixture of C1–C5 linear alkanes, the long alkane adsorption first increases and then decreases with increasing pressure, but the short alkane adsorption is continuously increasing and progressively replaces the long alkanes at high pressures due to the size entropy effect. This phenomenon was already detected before in Refs. [20, 21] for silicalite and by Heyden *et al.* [22] for binary mixtures of methane, ethane, propane, and tetrafluoromethane in SWCNTs by using CBMC simulations. At high loadings, a maximum occurs with increasing pressure in the absolute adsorption isotherm of one or both adsorbing species. It was detected that there exist two fundamentally different reasons for this maximum. First, the size entropy effect [23] and second, non-ideality effects of the gas phase [22] can be made responsible for this maximum. If, owing to non-ideality effects of the gas phase, the fugacity of one component does not increase as steeply with pressure as the other component, a maximum can occur in the absolute adsorption isotherm of this component [22]. It must be stressed that the displaced component is not necessarily the larger molecule. Similar effects were also observed by Jakobtorweihen *et al.* [24] for

1
2
3
4
5
6
7
8
9
10
11
12
13
14
15
16
17
18
19
20
21
22
23
24
25
26
27
28
29
30
31
32
33
34
35
36
37
38
39
40
41
42
43
44
45
46
47
48
49
50
51
52
53
54
55
56
57
58
59
60

adsorption of alkenes in various zeolites.

Kondratyuk *et al.* [5] found three well-defined adsorption sites on opened single-walled carbon nanotubes (tube diameter 13.6 Å) by temperature programmed desorption measurements for several alkanes. On the basis of hybrid Monte Carlo simulations, the two highest binding energy adsorption site correspond to adsorption inside tubes, and to groove sites between adjacent nanotubes in bundles. The third highest binding energy corresponds to sites on the exterior nanotube surface. Burde *et al.* [2] investigated the kinetics of gas uptake on different regions of carbon nanotube bundles by means of the kinetic Monte Carlo scheme. On both external and internal sites of a nanotube bundle, equilibration times are observed to decrease linearly as the coverage increases toward monolayer completion; the rate at which this occurs strongly depends on the ratio between the binding energy and the temperature. For low coverages, very long equilibration times can be observed. The adsorption in pore-like phases is typically 2 orders of magnitude slower than that of external phases.

A survey of computational techniques for carbon nanotubes was presented by Rafii-Tabar [25].

The motivation of the this paper is the investigation of alkene adsorption in SWCNTs and the separation potential of **linear** alkanes and alkenes in carbon nanotubes. Furthermore, the effect of pore diameters on adsorption and the adsorption in the interstitial space in CNT-bundles is evaluated. **Hysteresis is not investigated in this work. Jiang *et al.* [6] have found hysteresis for alkane adsorption inside a CNT having a larger diameter as the widest pore employed in this study, but the dependence of hysteresis on tube size was not studied.**

The outline of this article is as follows: In the next section the models underlying our simulations are explained and details of the simulations are given. In section 3, the results are shown and discussed. We end with a conclusion in the last section.

2. SIMULATION DETAILS

Intermolecular interactions were modelled with the truncated Lennard-Jones (LJ) 12-6 potential. The fluid molecules were modelled as united-atoms. For the intramolecular and the fluid-fluid intermolecular interactions the TraPPE force field was used [26, 27], where the bond angle bending is described by a harmonic potential and

Table 1. Lennard-Jones parameters and their source.

| centre | σ [Å] | ϵ/k_B [K] | Ref. |
|------------------------------------|--------------|--------------------|------|
| CH ₄ | 3.73 | 148 | [26] |
| CH ₃ (sp ³) | 3.75 | 98 | [26] |
| CH ₂ (sp ³) | 3.95 | 46 | [26] |
| CH ₂ (sp ²) | 3.675 | 85 | [27] |
| CH(sp ²) | 3.73 | 47 | [27] |
| carbon | 3.4 | 28 | [28] |

the bond torsion with a 3-cosine-fourier potential. For *trans*- and *cis*-2-butene an harmonic torsional potential is used. In the TraPPE force field the bond lengths are fixed. To check the influence of this assumption, some systems were re-simulated with an harmonic bond potential, we found no influence on the adsorption isotherms.

The carbon LJ parameters were taken from Ref. [28]. Lorentz-Berthelot mixing rules were used to determine the interactions of unlike molecular centres. The LJ parameters are listed in table 1. For the LJ interactions a cutoff radius of 14 Å was used in combination with the usual tail corrections [29]. Note that Macedonia and Maginn [30] have shown that tail corrections do not apply to adsorption in nanoporous materials as tail corrections assume a homogenous distribution of the molecules behind the cutoff. As the TraPPE force field includes tail corrections and to date no force field that was explicitly developed for hydrocarbon-CNT interactions is available (lack of experimental data prevent developing such parameters), tail corrections were used in this study. Moreover, Macedonia and Maginn [30] have shown that the influence of tail correction on calculated adsorption isotherms for butane in silicalite is small. The influence on the systems studied in this work is also minor. For example, ethane at a temperature of 300 K and a pressure of 1 bar inside a (20,0) CNT shows an adsorption capacity of 3.69 mol/kg, this value reduces to 3.34 mol/kg when tail corrections are not used.

The size and helicity of carbon nanotubes is specified by two integer numbers [31] n_1 and n_2 , so they can be unambiguously labelled as (n_1, n_2) . All results in this work were obtained with single-walled carbon nanotubes in a zigzag structure. For $n_2=0$ tubes have the zigzag

1
2
3 structure, at which one carbon-carbon bond is parallel to the pore axis. The investigated
4 tubes have the following inner diameters: 7.8 Å (10,0), 15.7 Å (20,0), 23.5 Å (30,0), and 31.3
5 Å (40,0). Note that, although deformations can occur especially for larger tubes, we have
6 simulated all nanotubes as “perfect” single-walled nanotubes. As framework flexibility has a
7 vanishing influence on adsorption isotherms [32] we modelled the nanotubes as rigid (carbon
8 atoms fixed on their positions). Note that carbon nanotube flexibility can have a dramatic
9 influence on the dynamics of guest molecules [33]. The rigid framework assumption allows
10 the use of interpolation grids for the calculation of the fluid-nanotube interactions. A grid
11 fineness of 0.065 Å was used. The nanotubes length was set to 102 Å. However, effectively
12 an infinitely long tube was simulated as usual periodic boundaries [34] were used for the
13 direction parallel to the pore axis.

14
15 Grand canonical Monte Carlo simulations were performed to calculate adsorption
16 isotherms. In the grand canonical ensemble the number of particles can fluctuate
17 whereas the chemical potentials, the temperature, and the volume are constant. For
18 details about the GCMC method see Ref [29]. For effective simulations of molecules
19 the configurational bias Monte Carlo method was used, which allows the growth of
20 a molecule atom by atom [35, 36]. The following Monte Carlo trials were performed
21 during a GCMC simulations: displacement of a molecule, rotation of a molecule
22 around its centre of mass, partial and total regrowth of a molecule, and molecule
23 exchange with a reservoir. Additionally, for simulating mixtures particle identity
24 changes were carried out. All acceptance rules are summarised in an earlier publication [37].
25
26
27
28
29
30
31
32
33
34
35
36
37
38
39
40
41
42
43
44
45
46
47
48
49
50
51
52
53
54
55
56
57
58
59
60

The number of generated configurations depends on the system. For all studied systems more than 1.5 million Monte Carlo trials were performed for equilibration and more than 8 million trials were carried out for sampling. For the molecule exchange acceptance rules either the bulk chemical potentials or the bulk fugacities must be specified [37]. The fugacities were calculated with the Peng-Robinson equation of state using parameters taken from Ref [38]. To determine the Henry coefficients and the isosteric heats of adsorption Monte Carlo simulations in the canonical ensemble in combination with the CBMC technique were carried out for the zero loading limit [39] (only one fluid molecule). Additionally, a separate simulation in the ideal gas state was necessary. The Henry coefficient can then be calculated as

$$K_H = \beta \frac{\langle \mathcal{W} \rangle}{\langle \mathcal{W}_{IG} \rangle}, \quad (1)$$

where $\beta = 1/(k_B T)$ and \mathcal{W} is the normalised Rosenbluth factor calculated according to the CBMC approach [29, 35, 36]. The subscript, IG, is used to indicate the ideal gas state. The angular brackets denote ensemble averages. The term k_B is the Boltzmann constant and T the temperature. The isosteric heat of adsorption has been calculated from

$$q_{st}^0 = \langle U \rangle_{IG} - \langle U \rangle + k_B T, \quad (2)$$

where U is the total energy.

3. RESULTS AND DISCUSSION

The first results in this section are for adsorption inside a single carbon nanotubes, thereafter results for CNT bundles are shown. All presented isotherms are absolute adsorption isotherms.

The pure component adsorption isotherms are presented by plotting the amount of moles adsorbed per unit weight of adsorbent as a function of pressure. Error bars have not been included in the figures since they are, in almost all cases, smaller than the symbols. In figures 1 and 2 the pure component adsorption isotherms of ethane, ethene, propane, and propene for various single-walled carbon nanotubes at 300 K are presented.

As can be seen from figure 1, at low pressures more alkane molecules are adsorbed than alkenes, and the adsorption in narrow pores is stronger than in wider pores. The interaction of the adsorbed molecules is stronger in narrow pores, and the isotherms level off at lower pressures than in larger pores. As expected, at higher pressures more molecules can be

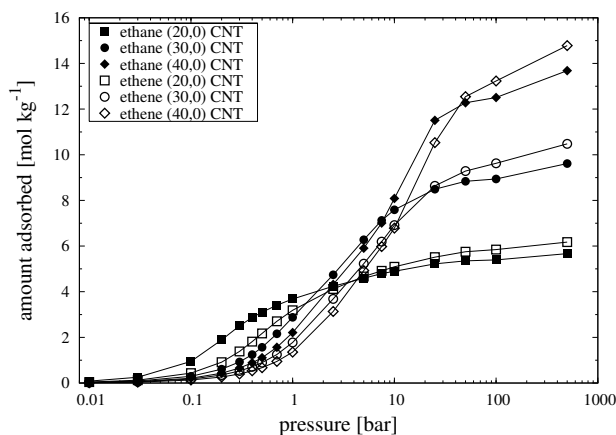


Figure 1. Adsorption isotherms of ethane and ethene in different carbon nanotubes at 300 K. Lines are added to guide the eye.

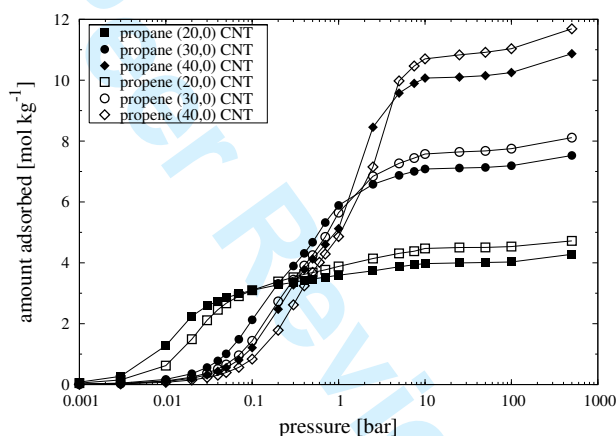


Figure 2. Adsorption isotherms of propane and propene in different carbon nanotubes at 300 K. Lines are added to guide the eye.

adsorbed inside the larger pores. A comparison between figures 1 and 2 shows that at low pressures more propane molecules are adsorbed than ethane, but at high pressure the number of adsorbed ethane molecules is higher as the required space is smaller than for propane. At low pressures both ethene and propene are adsorbed in a smaller amount than the respective alkanes, at high pressures it is the opposite. This is caused by the larger number of interaction sites of alkanes. At high pressure the smaller size of alkenes is decisive.

In figure 3 the adsorption isotherms of 1-butene, *cis*-butene, and *trans*-butene at 300 K in (20,0) and (40,0) SWCNTs are presented. As before, at low pressures more molecules in the narrow pores are adsorbed, and at high pressure it is the opposite. The adsorption

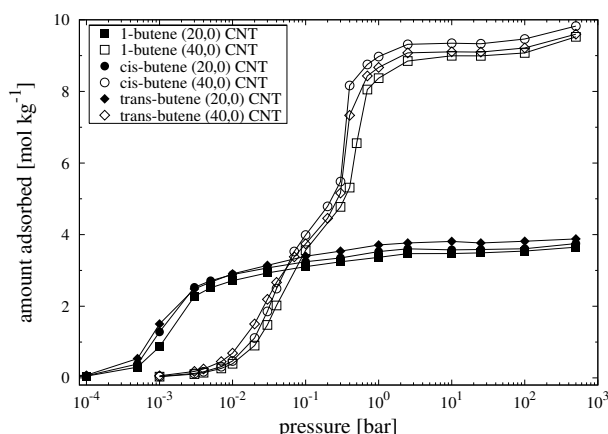


Figure 3. Adsorption isotherms of 1-butene, *cis*-2-butene, and *trans*-2-butene in different carbon nanotubes at 300 K. Lines are added to guide the eye.

behaviour of the three alkenes is quite similar.

The development of adsorption layers for 1-butene is shown in detail in figure 4. RD profiles of 1-butene inside a (40,0) SWCNT at 300 K and four pressures (0.1, 0.4, 0.6, and 100 bar) are presented. Additionally, the adsorption isotherm is given, where the state point for which the RD profile is shown is marked with a cross. At 0.1 bar the first adsorption layer, at a distance of 0.4 nm from the wall, is formed. At a slightly higher pressure of 0.4 bar the formation of a second layer is initiated. The centre part of the tube (1.2–1.6 nm) is still empty. This changes at 0.6 bar where the third layer is slowly built up and the second layer gets more distinctive. Eventually, at 100 bar the third layer is formed and the centre part of the tube is filled.

Figure 5 shows the calculated Henry coefficients of *n*-alkanes as a function of their carbon numbers at 300 K in SWCNTs of various diameters. These simulations were executed for the zero loading limit. The very strong interaction between the (10,0) carbon nanotube and the alkanes is demonstrated by the rather large Henry coefficients compared to the values for the wider tubes. The alkenes (see figure 6) show a similar behaviour. A comparison of the Henry coefficients of 1-butene, *cis*-2-butene, and *trans*-2-butene in (10,0) carbon tubes reveals that *trans*-2-butene adsorbs strongest and the comparatively bulky *cis*-2-butene adsorbs weakest.

For both alkanes and alkenes the differences between the Henry coefficients become smaller the larger the tube diameters are. This is also supported by the isosteric heats of adsorption in figures 7 and 8. The heats of adsorption show a linear dependence on the

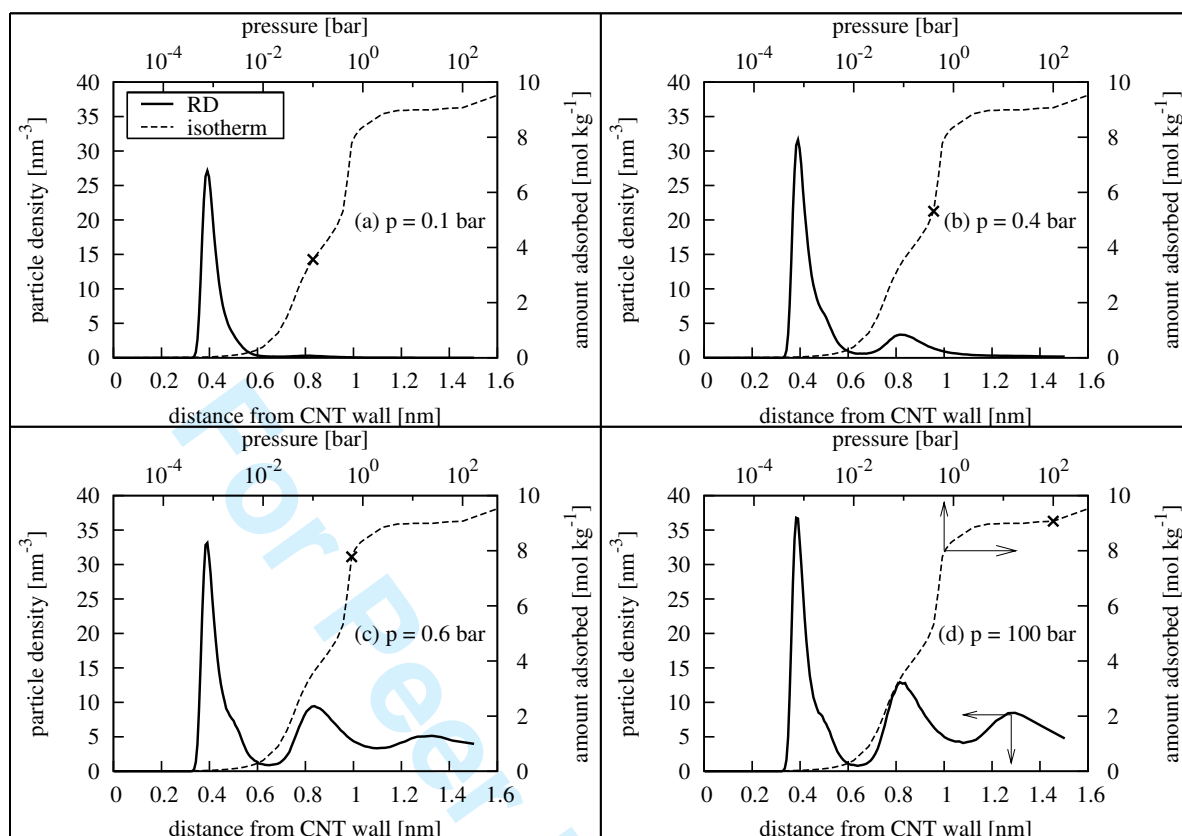


Figure 4. Radial density (RD) profiles represent 1-butene distributions inside a (40,0) CNT at 300 K. The adsorption isotherm of 1-butene at 300 K is plotted on the secondary axes, the state point for which the RD profile is shown is marked with a cross. RD profiles for four different pressures are shown: (a) 0.1 bar, (b) 0.4 bar, (c) 0.6 bar, and (d) 100 bar.

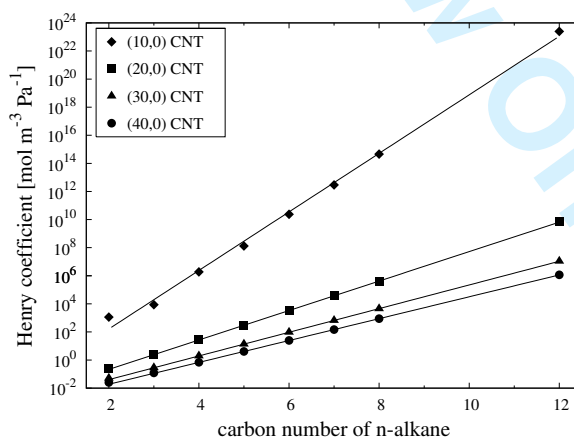


Figure 5. Henry coefficients of *n*-alkanes as functions of their carbon numbers at 300 K in different carbon nanotubes. Lines represent exponential fits.

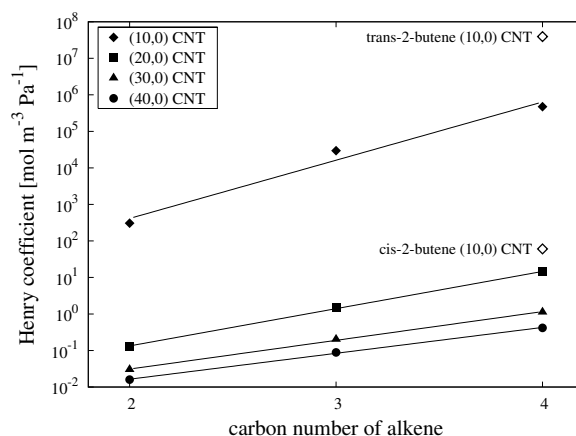


Figure 6. Henry coefficients of alkenes as functions of their carbon numbers at 300 K in different carbon nanotubes. Lines represent exponential fits. Additionally, the results for *cis*-2-butene and *trans*-2-butene in the (10,0) carbon nanotube are shown (open symbols).

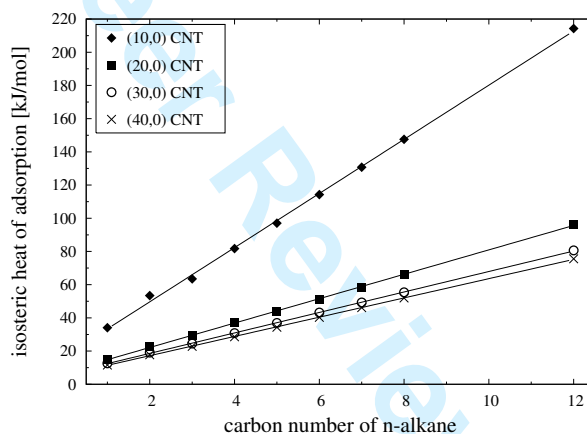


Figure 7. Isosteric heats of adsorption of *n*-alkanes as function of their carbon numbers for the zero loading limit at 300 K in different carbon nanotubes. Lines represent linear fits.

chain length for alkanes and alkenes. Note that both, the chain length dependency of the Henry coefficients and the chain length dependency of the heats of adsorption were also observed experimentally for alkanes in zeolites [40]. Furthermore, these dependencies were already observed with molecular simulation methods for the adsorption of alkanes in CNT bundles [4] and, in agreement with experiments, for the adsorption in silicalite [20, 41].

In table 2 a comparison of Henry coefficients, K_H , and isosteric heats of adsorption, q_{st} , for the butenes inside carbon nanotubes of different sizes is presented. Unlike the (10,0) tube (see also figures 6 and 8), the larger nanotubes show the following sequence in the K_H

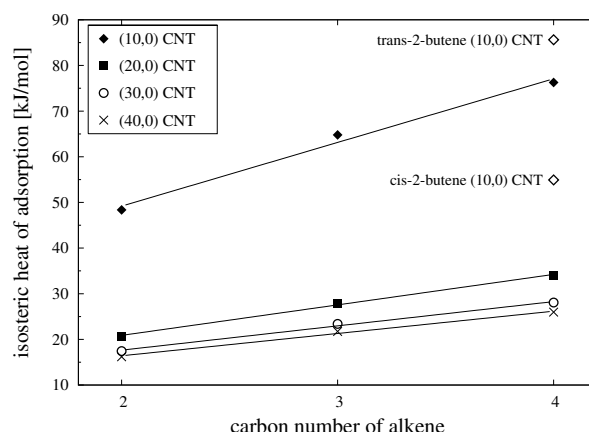


Figure 8. Isosteric heats of adsorption of alkenes as function of their carbon numbers for the zero loading limit at 300 K in different carbon nanotubes. Lines represent linear fits. Additionally, the results for *cis*-2-butene and *trans*-2-butene in the (10,0) carbon nanotube are shown (open symbols).

and q_{st} values: 1-butene < *cis*-2-butene < *trans*-2-butene. In the (10,0) nanotube the order is *cis*-2-butene < 1-butene < *trans*-2-butene. In the narrow (10,0) tube the structure of the 1-butene molecule is changed compared to the structure in the ideal gas state, whereas the structure of 1-butene in the wider tubes is similar to the structure in the ideal gas state. The structure of 1-butene in a (10,0) CNT is closer to *trans*-2-butene than in the other tubes. Moreover, in the (10,0) nanotube 1-butene is never in the *cis* state, whereas in the ideal gas state a small fraction of 1-butene molecules can be found in the *cis* configuration. Thus, the 1-butene molecule structure is adjusted to better fit these molecules into the narrow channels.

For silicalite-1 and highly de-aluminated Y zeolite (US-Ex), Thamm *et al.* [42] found a linear relation between the experimental initial heats of adsorption of *n*-alkanes and cyclohexane and their critical parameters

$$q_{st}^0 = D \frac{T_C}{p_C^{0.5}}, \quad (3)$$

where D represents the proportional constant. These authors showed that the isosteric heat of adsorption of ethene and 1-butene is also determined by this relation. Jakobtorweihen *et al.* [24] confirmed these findings by simulations of a broad variety of alkanes and alkenes in silicalite-1. Bruce *et al.* [43] found this result also for graphitized black powders. In figure 9 the relation given in equation 3 is confirmed for linear alkanes and some alkenes

Table 2. Comparison of the Henry coefficients, K_H , and the isosteric heats of adsorption, q_{st} , for the butenes in different carbon nanotubes. All results correspond to a temperature of 300 K. Errors are given in the subscripts.

| species | CNT | K_H | q_{st} |
|------------------------|--------|--|-------------------------|
| | | [mol m ³ Pa ⁻¹] | [kJ mol ⁻¹] |
| 1-butene | (10,0) | 4.733×10 ⁵ _{0.158} | 76.26 _{0.04} |
| <i>cis</i> -2-butene | (10,0) | 6.047×10 ¹ _{0.603} | 54.92 _{0.10} |
| <i>trans</i> -2-butene | (10,0) | 3.938×10 ⁷ _{0.071} | 85.62 _{0.03} |
| 1-butene | (20,0) | 14.214 _{0.027} | 34.04 _{0.01} |
| <i>cis</i> -2-butene | (20,0) | 16.694 _{0.051} | 35.37 _{0.01} |
| <i>trans</i> -2-butene | (20,0) | 22.092 _{0.055} | 36.36 _{0.02} |
| 1-butene | (30,0) | 1.127 _{0.002} | 28.07 _{0.01} |
| <i>cis</i> -2-butene | (30,0) | 1.319 _{0.004} | 29.48 _{0.02} |
| <i>trans</i> -2-butene | (30,0) | 1.879 _{0.006} | 30.72 _{0.01} |
| 1-butene | (40,0) | 0.417 _{0.001} | 25.97 _{0.01} |
| <i>cis</i> -2-butene | (40,0) | 0.486 _{0.001} | 27.34 _{0.02} |
| <i>trans</i> -2-butene | (40,0) | 0.691 _{0.002} | 28.64 _{0.02} |

in SWCNTs of various diameters. Only the bulky *cis*-2-butene shows a somewhat larger deviation in the very narrow (10,0) tube.

In figure 10a simulated adsorption isotherms of the binary mixture of ethane and ethene inside a (20,0) carbon nanotube at 300 K for a fixed equimolar bulk phase composition are presented. Additionally the selectivity is shown. The selectivity of component 1 with respect to component 2 is defined as

$$S_{12} = \frac{x_1/y_1}{x_2/y_2}, \quad (4)$$

where x and y are the mole fractions of the adsorbed phase and the bulk phase, respectively. The lines represent results obtained by the ideal adsorption solution theory (IAST) [44]. For these calculations the pure component adsorption isotherms detailed in this work were used. To take into account the non-ideality of the gas phase, we have used the

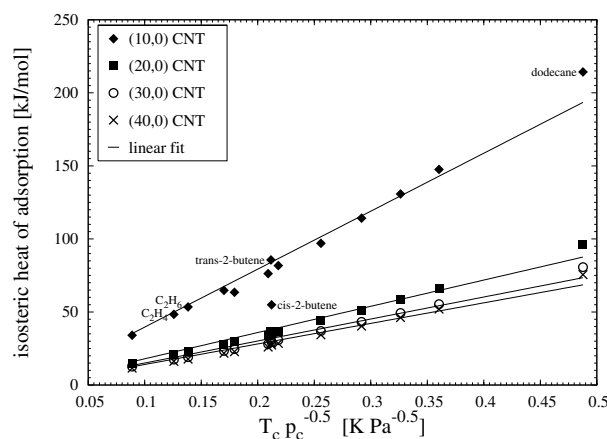


Figure 9. Dependence of the simulated isosteric heats of adsorption for the zero loading limit at 300 K in different carbon nanotubes on the critical data for hydrocarbons. Lines represent linear fits, where the fit constants are: $D_{10}=396.64$, $D_{20}=179.66$, $D_{30}=150.66$, and $D_{40}=140.66$.

fugacities rather than the pressure for calculating the IAST isotherms. Like for the pure component adsorption, at low pressure more ethane than ethene is adsorbed. At high pressures the entropic effect [23] leads to a reversal. Thus, we observe a distinct maximum in the ethane isotherm, which is also calculated by the IAST. A further reason for the maximum of the isotherms is a non-ideality effect of the gas phase. Details are given by Heyden *et al.* [22]. In figure 10b the component fugacities of ethane and ethene in the gas phase as calculated by the Peng-Robinson equation of state show a difference between the fugacities from about 25 bar on. Close to this value is the maximum of the adsorption isotherm of ethane. These maxima were also observed by Jiang *et al.* [4] and Heyden *et al.* [22] for carbon nanotubes and by Jakobtorweihen *et al.* [24] for zeolites, among others. Note that Jiang *et al.* [4] have also observed distinct maxima in the selectivities for mixtures of C5 isomers.

The selectivity drops from about two at low pressures to about one at high pressures.

A qualitatively similar behaviour can be observed in figure 11 for a propane and propene binary mixture. The selectivities for this mixture are closer to one. The larger the hydrocarbons the weaker the influence of the double bond. Hence, the higher the carbon number the higher the similarity of an alkane and an 1-alkene having the same carbon number. It can be concluded, that for these kind of alkane-alkene mixtures the separation is more difficult the higher the carbon number.

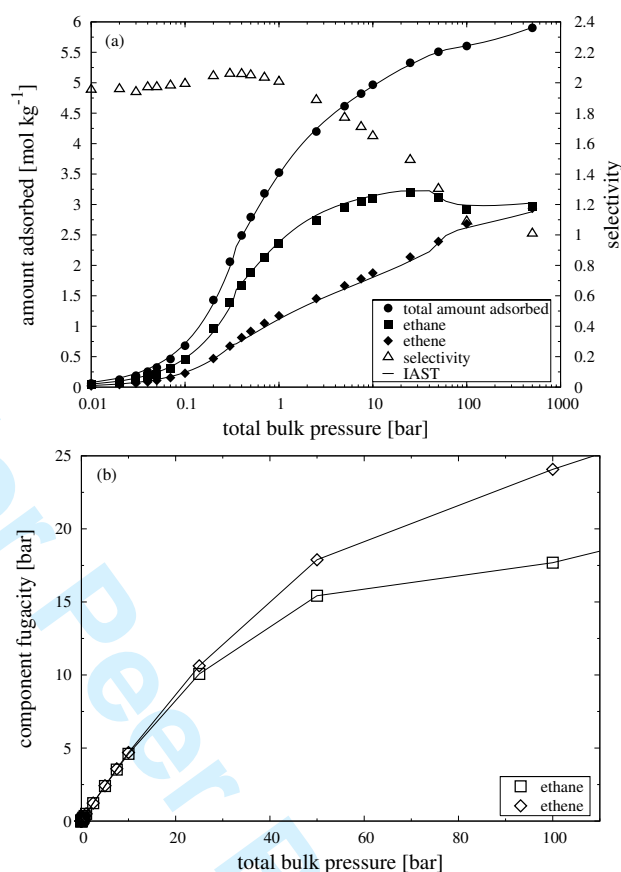


Figure 10. (a) Simulated adsorption isotherm of a binary mixture of ethane and ethene inside a (20,0) carbon nanotube for a fixed equimolar bulk phase composition at 300 K and selectivity of ethane with respect to ethene. Lines represent results of the ideal adsorption solution theory. (b) The corresponding component fugacities, calculated with the Peng-Robinson equation of state, are plotted against total bulk pressure. Lines are added to guide the eye.

Figure 12 shows the adsorption isotherms of *cis*-2-butene and *trans*-2-butene inside a (20,0) SWCNT at 400 K for a fixed equimolar bulk phase composition. The lines present again the IAST results. Initially the adsorption isotherms are very similar. At very high pressures a configurational entropic effect occurs and the isotherms start to diverge. An effective separation of these isomers is therefore, if at all, only possible at very high pressures. A better separation can be achieved for a binary mixture of propane and 1-butene (see figure 13).

All results presented above dealt with adsorption inside, and only inside, a single CNT.

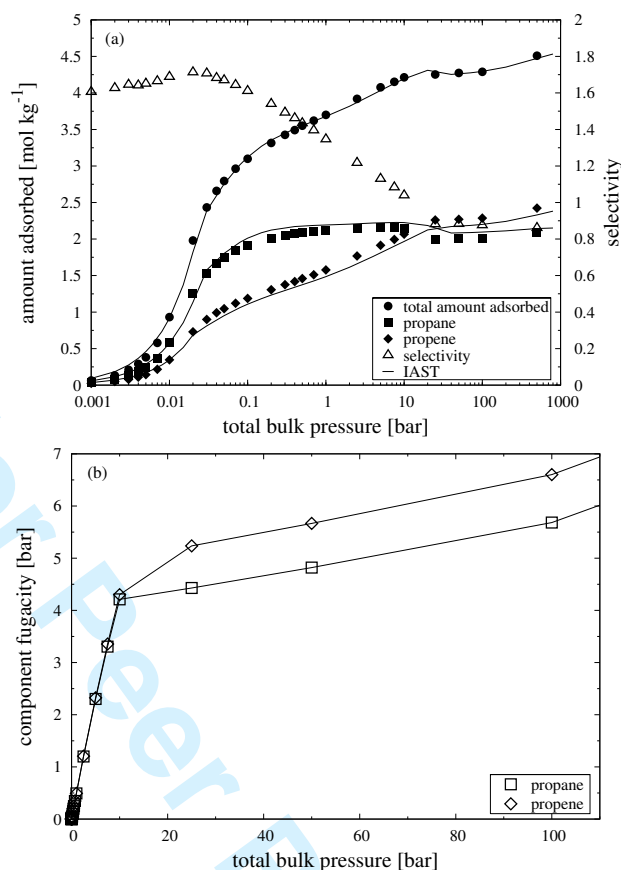


Figure 11. (a) Simulated adsorption isotherm of a binary mixture of propane and propene inside a (20,0) carbon nanotube for a fixed equimolar bulk phase composition at 300 K and selectivity of propane with respect to propene. Lines represent results of the ideal adsorption solution theory. (b) The corresponding component fugacities, calculated with the Peng-Robinson equation of state, are plotted against total bulk pressure. Lines are added to guide the eye.

In order to investigate the adsorption in the interstitial space of bundles of SWCNTs, hexagonally arranged bundles of SWCNTs with various diameters were investigated. The distance a (see figure 14) was set to 0.36 nm. In figure 15 the fraction of ethane molecules located in the interstitial space of different SWCNT bundles at 300 K is shown.

As the interstitial space is small, no ethane molecules adsorb in the interstitial space of (10,0) tubes in a hexagonal arrangement. Inside (20,0) tubes the interstitial space is just large enough to adsorb ethane molecules (see figure 16), but a pressure of at least 1 bar is necessary to initiate a measurable adsorption.

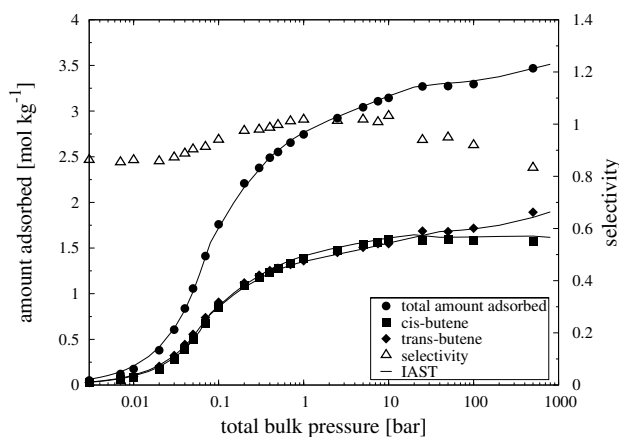


Figure 12. Simulated adsorption isotherm of a binary mixture of *cis*-butene and *trans*-butene inside a (20,0) carbon nanotube for a fixed equimolar bulk phase composition at 400 K and selectivity of *cis*-butene with respect to *trans*-butene. Lines represent results of the ideal adsorption solution theory.

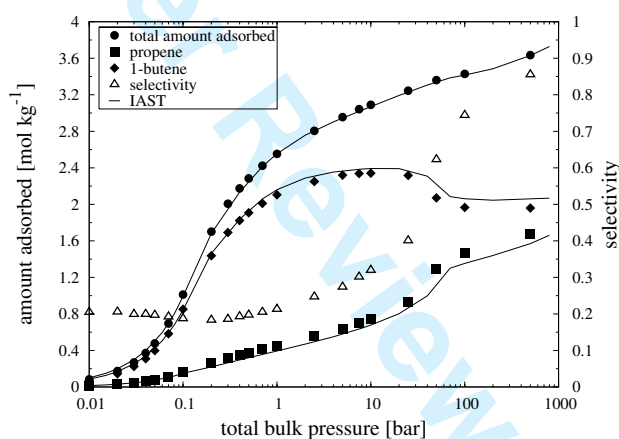


Figure 13. Simulated adsorption isotherm of a binary mixture of propene and 1-butene inside a (20,0) carbon nanotube for a fixed equimolar bulk phase composition at 400 K and selectivity of propene with respect to 1-butene. Lines represent results of the ideal adsorption solution theory.

For the (30,0) and (40,0) tubes in hexagonal arrangement, ethane molecules at low pressure preferentially adsorb in the interstitial space. Due to the wall surrounding this is the energetically most favourable position (see also figure 16). From about 0.01 bar on, the interstitial space for (30,0) and (40,0) tubes in hexagonal arrangement are nearly filled, and adsorption inside the tubes starts (see figure 15).

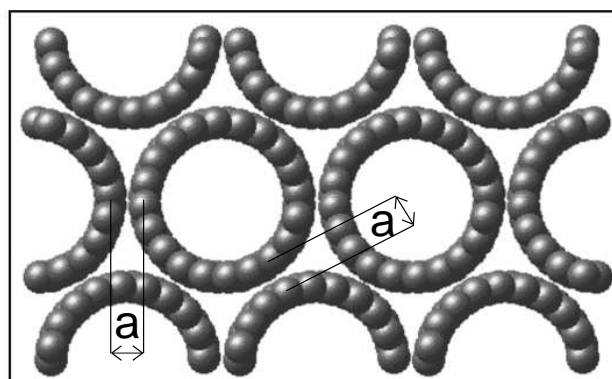


Figure 14. Carbon nanotubes in a hexagonally arranged bundle. The x - y plan of the bundle of (20,0) nanotubes are shown as it was used in the simulations. For all investigated bundles a was set to 0.36 nm.

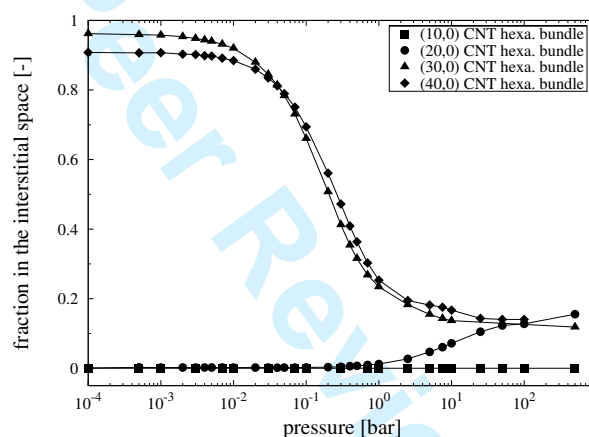


Figure 15. Fraction of ethane located in the interstitial space of a hexagonally arranged carbon nanotube bundle at a temperature of 300 K. All bundles contain only one type of nanotubes. Lines are added to guide the eye.

In this study the distance of the tubes $a=0.36$ nm (see figure 14) was chosen according to the employed force field parameters ($\sigma_C=0.34$ nm and the position of the minimum $2^{1/6}\sigma_C=0.38$ nm). Note that in other studies [45] the tube-tube distance is revealed to be smaller than 0.36 nm. Whether or not ethane adsorbs in the interstitial space is strongly dependent on the tube-tube distances and the nanotube radii.

However, the recently produced CNT-membranes contain CNTs encapsulated in a matrix [46, 47], so that the interstitial space is not accessible for adsorption. Note that for a comparison between measured adsorption isotherms and simulations the real tube diameters

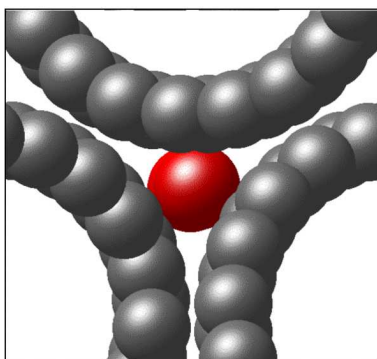


Figure 16. The snapshot displays an ethane molecule in the interstitial space of a hexagonal arranged bundle of (20,0) carbon nanotubes.

and tube arrangements are needed. Furthermore, the tubes have to be open at both ends which was obviously not always the case in previous measurements [48].

4. CONCLUSION

Molecular simulations have been performed to evaluate the adsorption isotherms of linear alkanes, alkenes, and some of their binary mixtures. As expected, at low pressures the adsorption in narrow pores is stronger than in wider pores, and more alkanes than alkenes are adsorbed under these conditions. At higher pressures more molecules inside larger pores can be adsorbed. At low pressures more alkanes are adsorbed than the corresponding alkenes, at high pressures it is the opposite. Short and long alkanes show, in principle, the same adsorption isotherm shapes. The adsorption isotherms of 1-butene, *cis*-2-butene, and *trans*-2-butene are quite similar. The Henry coefficients and isosteric heats of adsorption of all alkanes and alkenes investigated revealed a very strong interaction with the (10,0) CNT ($d_{CNT}=7.8 \text{ \AA}$). For both alkanes and alkenes the differences between the Henry coefficients and isosteric heats of adsorption become smaller the larger the tube diameters are. The relation between critical parameters and the isosteric heats of adsorption by Thamm *et al.* [42] could be confirmed for adsorption in CNTs. For each of the binary mixtures, one component isotherm shows a distinct maximum. This could be attributed to a configurational entropy effect inside the pores and non-idealities in the bulk phase. The IAST calculations also showed these maxima, and coincided with the simulation results. The selectivity of the ethane-ethene mixture is higher at low pressures than for propane-propene. *Cis*- and *trans*-

1
2
3 2-butene can only be separated, if at all, at very high pressures. The larger the difference in
4 the carbon numbers of the co-adsorbing species the larger the selectivity. The selectivities
5 are low when both components (*n*-alkane and 1-alkene) have the same number of carbons.
6
7 At low pressures, a considerable amount of ethane is adsorbed in the interstitial space of
8 the here investigated hexagonal arrangements (tube-tube distance $a=0.36$ nm) of (30,0) and
9 (40,0) CNTs.
10
11

12
13
14 **Acknowledgment.** This work was supported by the Deutsche Forschungsgemeinschaft
15 (DFG) in priority program SPP 1155. We thank Niels Hansen for help with IAST calcula-
16 tions.
17
18
19
20
21
22
23
24
25
26
27
28
29
30
31
32
33
34
35
36
37
38
39
40
41
42
43
44
45
46
47
48
49
50
51
52
53
54
55
56
57
58
59
60

-
- 1
2
3
4
5
6
7 [1] S. Iijima, *Helical microtubules of graphitic carbon*, Nature, 354 (1991), pp. 56–58.
8
9 [2] J. T. Burde and M. M. Calbi, *Physisorption kinetics in carbon nanotube bundles*, J. Phys.
10 Chem. C, 111 (2007), p. 5057.
11
12 [3] D. Cao, X. Zhang, J. Chen, W. Wang, and J. Yun, *Optimization of single-walled carbon*
13 *nanotube arrays for methane storage at room temperature*, J. Phys. Chem. B, 107 (2003), p.
14 13286.
15
16 [4] J. Jiang, S. I. Sandler, M. Schenk, and B. Smit, *Adsorption and separation of linear and*
17 *branched alkanes on carbon nanotube bundles from configurational-bias monte carlo simulation*,
18 Phys. Rev. B, 72 (2005), p. 045447.
19
20 [5] P. Kondratyuk, Y. Wang, J. K. Johnson, and J. T. Yates, *Observation of a one-dimensional*
21 *adsorption site on carbon nanotubes: Adsorption of alkanes of different molecular lengths*, J.
22 Phys. Chem. B, 109 (2005), p. 20999.
23
24 [6] J. Jiang, S. I. Sandler, and B. Smit, *Capillary phase transitions of n-alkanes in a carbon*
25 *nanotube*, Nano Letters, 4 (2004), pp. 241–244.
26
27 [7] F. Darkim, P. Melbrunot, and G. P. Tartaglia, *Review of hydrogen storage by adsorption in*
28 *carbon nanotubes*, Int. J. Hydrogen Energy, 27 (2002), p. 193.
29
30 [8] V. Meregalli and M. Parinello, *Review of theoretical calculations of hydrogen storage in carbon-*
31 *based materials*, Appl. Phys. A, 72 (2001), p. 143.
32
33 [9] G. Froudakis, *Hydrogen interaction with carbon nanotubes: a review of ab initio studies*, J.
34 Phys. Condens. Matter, 14 (2002), pp. R453–R465.
35
36 [10] J. I. Paredes, F. Suárez-García, S. Villar-Rodil, A. Martínez-Alonso, J. M. D. Tascón, and
37 E. J. Bottani, *n₂ physisorption on carbon nanotubes: Computer simulation and experimental*
38 *results*, J. Phys. Chem. B, 107 (2003), pp. 8905–8916.
39
40 [11] J. Jiang and S. I. Sandler, *Nitrogen adsorption on carbon nanotube bundles: Role of the*
41 *external surface*, Phys. Rev. B, 68 (2003), p. 245412.
42
43 [12] J. Jiang, N. J. Wagner, and S. I. Sandler, *A monte carlo simulation study of the effect of carbon*
44 *topology on nitrogen adsorption on graphite, a nanotube bundle, c₆₀ fullerite, c₁₆₈ schwarzite,*
45 *and a nanoporous carbon*, Phys. Chem. Chem. Phys., 6 (2004), pp. 4440–4444.
46
47 [13] G. Arora, N. J. Wagner, and S. I. Sandler, *Adsorption and diffusion of molecular nitrogen in*
48
49
50
51
52
53
54
55
56
57
58
59
60

- 1
2
3
4
5
6
7
8
9
10
11
12
13
14
15
16
17
18
19
20
21
22
23
24
25
26
27
28
29
30
31
32
33
34
35
36
37
38
39
40
41
42
43
44
45
46
47
48
49
50
51
52
53
54
55
56
57
58
59
60
- single wall carbon nanotubes*, *Langmuir*, 20 (2004), pp. 6268–6277.
- [14] J. Jiang and S. I. Sandler, *Nitrogen and oxygen mixture adsorption on carbon nanotube bundles from molecular simulation*, *Langmuir*, 20 (2004), p. 10910.
- [15] G. Arora and S. I. Sandler, *Air separation by single wall carbon nanotubes: Thermodynamics and adsorptive selectivity*, *J. Chem. Phys.*, 123 (2005), p. 044705.
- [16] A. Striolo, A. A. Chialvo, K. E. Gubbins, and P. T. Cummings, *Water in carbon nanotubes: Adsorption isotherms and thermodynamic properties from molecular simulation*, *J. Chem. Phys.*, 122 (2005), p. 234712.
- [17] M. C. Gordillo, L. Brualla, and S. Fantoni, *Neon adsorbed in carbon nanotube bundles*, *Phys. Rev. B*, 70 (2004), p. 245420.
- [18] B. Marcone, E. Orlandini, F. Toigo, and F. Ancilotto, *Condensation of helium in interstitial sites of carbon nanotubes bundles*, *Phys. Rev. B*, 74 (2006), p. 085415.
- [19] V. V. Simonyan, J. K. Johnson, A. Kuznetsova, and J. T. Yates, *Molecular simulation of xenon adsorption on single-walled carbon nanotubes*, *J. Chem. Phys.*, 114 (2001), pp. 4180–4185.
- [20] T. J. H. Vlugt, R. Krishna, and B. Smit, *Molecular simulations of adsorption isotherms for linear and branched alkanes and their mixtures in silicalite*, *J. Phys. Chem. B*, 103 (1999), pp. 1102–1118.
- [21] Z. Du, G. Manos, T. J. H. Vlugt, and B. Smit, *Molecular simulation of adsorption of short linear alkanes and their mixtures in silicalite*, *AIChE J.*, 44 (1998), pp. 1756–1764.
- [22] A. Heyden, T. Düren, and F. J. Keil, *Study of molecular shape and non-ideality effects on mixture adsorption isotherms of small molecules in carbon nanotubes: A grand canonical monte carlo simulation study*, *Chem. Eng. Sci.*, 57 (2002), pp. 2439–2448.
- [23] M. Schenk, S. L. Vidal, T. J. H. Vlugt, B. Smit, and R. Krishna, *Separation of alkane isomers by exploiting entropy effects during adsorption on silicalite-1: A configurational-bias monte carlo simulation study*, *Langmuir*, 17 (2001), pp. 1558–1570.
- [24] S. Jakobtorweihen, N. Hansen, and F. J. Keil, *Molecular simulation of alkene adsorption in zeolites*, *Molec. Phys.*, 103 (2005), pp. 471–489.
- [25] H. Rafii-Tabar, *Computational Physics of Carbon Nanotubes*, Cambridge University Press, Cambridge, 2008.
- [26] M. G. Martin and J. I. Siepmann, *Transferable potentials for phase equilibria. 1. United-atom description of n-alkanes*, *J. Phys. Chem. B*, 102 (1998), pp. 2569–2577.

- 1
2
3
4 [27] C. D. Wick, M. G. Martin, and J. I. Siepmann, *Transferable potentials for phase equilibria. 4.*
5 *United-atom description of linear and branched alkenes and alkylbenzenes*, J. Phys. Chem. B,
6 104 (2000), pp. 8008–8016.
7
8
9 [28] W. A. Steele, *The Interaction of Gases with Solid Surfaces*, Pergamon, Oxford, 1974.
10
11 [29] D. Frenkel and B. Smit, *Understanding Molecular Simulations, From Algorithms to Applica-*
12 *tions*, 2nd ed., Academic Press, San Diego, 2002.
13
14 [30] M. D. Macedonia and E. J. Maginn, *A biased grand canonical monte carlo method for simu-*
15 *lating adsorption using all-atom and branched united atom models*, Molec. Phys., 96 (1999),
16 pp. 1375–1390.
17
18 [31] R. Saito, M. Fujita, G. Dresselhaus, and M. S. Dresselhaus, *Electronic structure of chiral*
19 *graphene tubules*, Appl. Phys. Lett., 60 (1992), pp. 2204–2206.
20
21 [32] T. J. H. Vlugt and M. Schenk, *Influence of framework flexibility on the adsorption properties*
22 *of hydrocarbons in the zeolite silicalite*, J. Phys. Chem. B, 106 (2002), pp. 12757–12763.
23
24 [33] S. Jakobtorweihen, M. G. Verbeek, C. P. Lowe, F. J. Keil, and B. Smit, *Understanding*
25 *the loading dependence of self-diffusion in carbon nanotubes*, Phys. Rev. Lett., 95 (2005),
26 p. 044501.
27
28 [34] M. P. Allen and D. J. Tildesley, *Computer Simulation of Liquids*, Clarendon Press, Oxford,
29 1987.
30
31 [35] J. I. Siepmann and D. Frenkel, *Configurational bias monte carlo: a new sampling scheme for*
32 *flexible chains*, Molec. Phys., 75 (1992), pp. 59–70.
33
34 [36] D. Frenkel, G. Mooij, and B. Smit, *Novel scheme to study structural and thermal properties*
35 *of continuously deformable molecules*, J. Phys.: Condens Matter, 4 (1992), pp. 3053–3076.
36
37 [37] S. Jakobtorweihen, N. Hansen, and F. J. Keil, *Combining reactive and configurational-bias*
38 *monte carlo: Confinement influence on the propene metathesis reaction system in various*
39 *zeolites*, J. Chem. Phys., 125 (2006), p. 224709.
40
41 [38] B. E. Poling, J. M. Prausnitz, and J. P. O'Connell, *The Properties of Gases and Liquids*, 5th
42 ed., McGraw-Hill, New York, 2000.
43
44 [39] B. Smit and J. I. Siepmann, *Computer simulations of the energetics and sitting of n-alkanes*
45 *in zeolites*, J. Phys. Chem., 98 (1994), pp. 8442–8452.
46
47 [40] J. F. Denayer, W. Souverijns, P. A. Jacobs, J. A. Martens, and G. V. Baron, *High-temperature*
48 *low-pressure adsorption of branched c₅-c₈ alkanes on zeolite beta, zsm-5, zsm-22, zeolite y, and*
49
50
51
52
53
54
55
56
57
58
59
60

- 1
2
3 mordenite, *J. Phys. Chem. B*, 102 (1998), pp. 4588–4597.
4
5 [41] B. Smit and J. I. Siepmann, *Simulating the adsorption of alkanes in zeolites*, *Science*, 264
6 (1994), pp. 1118–1120.
7
8 [42] H. Thamm, H. Stach, and G. I. Berezin, *Anfangsadsorptionswärmen von Gasen und Dämpfen*
9 *an den SiO₂-Molekularsieben US-Ex und Silicalit*, *Z. Chem.*, 24 (1984), pp. 420–421.
10
11 [43] C. D. Bruce, T. R. Rybolt, H. E. Thomas, T. E. Agnew, and B. S. Davis, *Two-surface virial*
12 *analysis of alkane adsorption on carbopack c with and without hydrogen treatment*, *J. Colloid*
13 *Interface Sci.*, 194 (1997), pp. 448–454.
14
15 [44] A. L. Myers and J. M. Prausnitz, *Thermodynamics of mixed gas adsorption*, *AIChE J.*, 11
16 (1965), pp. 121–127.
17
18 [45] J.-C. Charlier, X. Gonze, and J.-P. Michenaud, *First-principles study of carbon nanotube*
19 *solid-state packings*, *Europhys. Lett.*, 29 (1995), pp. 43–48.
20
21 [46] J. K. Holt, H. G. Park, Y. wang, M. Stadermann, A. B. Artyukhin, C. P. Grigoropoulos,
22 A. Noy, and O. bakajin, *Fast mass transport through sub-2-nanometer carbon nanotubes*, *Sci-*
23 *ence*, 312 (2006), pp. 1034–1037.
24
25 [47] B. J. Hinds, N. Chopra, T. Rantell, R. Andrews, V. Gavalas, and L. G. Bachas, *Aligned*
26 *multiwalled carbon nanotube membranes*, *Science*, 303 (2004), pp. 62–65.
27
28 [48] S. Agnihotri and F.-L. Yun, *Fundamental structural properties of single-walled carbon nan-*
29 *otubes: Reopening the debate over hydrogen storage*, *AIChE Spring National Meeting, Con-*
30 *ference Proceedings*, American Institute of Chemical Engineers, New York, N.Y., 2006, p.
31 P43844.
32
33
34
35
36
37
38
39
40
41
42
43
44
45
46
47
48
49
50
51
52
53
54
55
56
57
58
59
60